Use of Half Metallic Heusler Alloys in CoFeB/MgO/Heusler Alloy Tunnel Junctions

P. J. Chen, G. Feng, and R. D. Shull

Magnetic Materials Group, National Institute of Standards and Technology, Gaithersburg, MD 20899-8552 USA

Heusler Alloys Co_2FeSi and Co_2MnSi were deposited on both single crystal MgO (100) and polycrystalline SiO_2 silicon thermal oxide substrates and characterized by x-ray diffraction before and after thermal annealing at various temperatures. Co_2FeSi and Co_2MnSi deposited on MgO (100) grow as $L2_1$ or B2 structures but grow as an A2 structure on the SiO_2 substrate. Co_2FeSi and Co_2MnSi were also deposited in a magnetic tunnel junction (MTJ) stack as the free and reference layers above and below the MgO barrier layer respectively, thereby replacing $Co_{20}Fe_{60}B_{20}$ as those layers in the more common MTJ stack. The tunneling magnetoresistance (TMR) ratio is higher if Co_2FeSi is the free layer, but lower when Co_2FeSi is the reference layer.

***Index Terms*—Co-based heusler alloys, magnetic tunnel junctions, MgO/CoFeB.**

I. Introduction

MAGNETIC tunnel junctions (MTJs) with MgO as the tunnel barrier have recently been widely studied. Their applications include magnetoresistive random access memory cells, read heads, magnetic field sensors, and spin torque oscillators. Two methods have been found to result in large tunneling magnetoresistance (TMR) values. One is to use half-metallic materials like Heusler alloys [1]–[3] which should have 100% spin polarized conduction electrons, on either side of the MgO. The other method is to use certain metals such as CoFe and CoFeB which have fully spin-polarized $\Delta 1$ Bloch states at the Fermi level, on either side of the MgO and take advantage of the coherent tunneling [4]–[7] possibility through the MgO provided by them. In addition, part of the attraction of half-metallic Heusler alloys is that they have high Curie temperatures, high spin polarizations and small magnetic damping constants. Thus, these materials are suitable for use in low power and high output spin-electronic devices. Heusler alloys have been predicted to exhibit half metallic ferromagnetic (HMF) behavior due to the presence of an energy gap for only one type of spin carrier at the Fermi level [8], [9]. Therefore, they are expected to have 100% spin polarization. In recent years, many experiments were performed to determine the magnetic properties of Heusler alloys because the spintronic effects will be larger in materials having a large spin polarization, thereby making applications easier. Many groups have successfully used different Heusler alloys in different MTJs stack structures. Successes to date include a high TMR values at room temperature of 217% measured by S. Tsunegi in a CoFe\MgO\$Co_2FeSi$ stack [10], 180% by E. Ozawa in a Co_2MnAl\MgO\CoFe stack [11], 340% by W. Wang in a Co_2FeAl\MgO\$Co_2FeAl$\CoFe [12] stack structure, 386% in stacks of $Co_2FeAl_{0.5}Si_{0.5}$\MgO\$Co_2FeAl_{0.5}Si_{0.5}$\CoFe [13] by N. Tezuka, 166% by Z. Wen for Co_2FeAl\MgO\CoFe [14], and 179% found by T. Ishikawa in stacks of C_o2MnSi/MgO/Co_2MnSi [15]. All these MTJ stacks were grown on MgO (100) substrates having a thick Cr seed layer to induce epitaxy. Since the seed layering requires a costly preanneal at high temperatures ($\approx 600\,^\circ C$), the present study was initiated to determine if that step could be eliminated, either by deposition directly onto single crystal MgO (100) or by growing the stacks on amorphous Si/SiO2 substrates which are compatible with the semiconductor industry.

In this paper, we will discuss the crystal structures resulting from depositing Co_2FeSi and Co_2MnSi on MgO(100) and SiO_2 substrates separately and the effect of that on the TMR ratio when placed in an MTJ stack with the Si/SiO_2 amorphous substrate.

II. Experimental Procedure

Our standard sample stack was as follows: Si\$SiO_2$ substrate\Ta(5 nm)\Ru(20 nm)\IrMn(7.5 nm)\CoFe(4 nm)\Ru(0.8 nm)\$Co_{20}Fe_{60}B_{20}$, Co_2FeSi or Co_2MnSi (3.5 nm)\MgO(2 nm)\$Co_{20}Fe_{60}B_{20}$,$Co_2FeSi$ or Co_2MnSi (4 nm)\Ta(5 nm)\Ru(10 nm) with the thicknesses of the layers enclosed in parentheses. All layers were grown in a multichamber deposition system with a base pressure of 6.6×10^{-7}Pa (5×10^{-9} torr). An argon gas pressure of 0.239 Pa (1.8 mtorr) was maintained during deposition. All layers were grown at room temperature. The MgO barrier layer was deposited by a RF magnetron sputtering gun from a MgO single crystal target while the other materials were deposited by DC magnetron sputtering. The Co_2FeSi and Co_2MnSi were deposited by cosputtering from pure Co, Fe, Mn and Si targets. The relative compositions of the Co_2FeSi and Co_2MnSi deposits were controlled by controlling the relative power of each sputtering gun, and the final compositions of the thin film deposits were determined by energy-dispersive x-ray scattering analysis (EDAX). The samples were subsequently annealed in vacuum at 360°C for 1 hour in the presence of an in-plane 398 kA/m (5 kOe) magnetic field to improve the crystallinity of the barrier and ferromagnetic layers.

We investigated the crystal structure of Co_2FeSi and Co_2MnSi deposited on either a MgO (100) single crystal substrate or a silicon thermal oxide substrate after deposition and after an annealing treatment (at various temperatures) by x-ray

Manuscript received November 05, 2012; revised January 09, 2013; accepted January 22, 2013. Date of current version July 15, 2013. Corresponding author: P. J. Chen (e-mail: peijie.chen@nist.gov).

Color versions of one or more of the figures in this paper are available online at http://ieeexplore.ieee.org.

Digital Object Identifier 10.1109/TMAG.2013.2244584

0018-9464/$31.00 © 2013 IEEE

diffraction (XRD) using Cu-Kα radiation. The sample stack for the x-ray characterization consisted of either (1) Si(001)\$SiO_2$ substrate \MgO(2 nm)\$Co_2FeSi$ or Co_2MnSi (55 nm)\MgO(5 nm), or (2) MgO(001) substrate \MgO(2 nm)\$Co_2FeSi$ or Co_2MnSi (55 nm)\MgO(5 nm). The bottom 2 nm of MgO was deposited as a seed layer and the top 5 nm of MgO was the capping layer. Grain sizes for a couple of the phases were also determined from the diffraction line widths and positions using the well known Scherrer relationship.

The TMR ratio of our samples was characterized by a current in plane testing (CIPT) system manufactured by Capres, Inc. [16]. All TMR values quoted in this report were measured at room temperature.

III. Results and Discussion

The XRD spectra of the as deposited and annealed Co_2FeSi and Co_2MnSi samples are shown in Figs. 1 and 2. In these spectra there are also a few peaks from the XRD sample holder and substrates. For instance, the Si (111) peak in the spectra is from the XRD sample holder, while the Si (004) peak is from the silicon thermal oxide substrate Si (001)\SiO_2 (300 nm). The MgO (002) peak is from the MgO single crystal substrate. In addition, the unlabeled diffraction line near 25 degrees is the Cu Kβ line for Si (111), and the line slightly higher is from a tungsten sample holder. Similarly, the unlabeled lines near 38 degrees and 62 degrees are the Cu Kβ diffraction lines for MgO (200) and Si (400) respectively. Other than the extra diffraction lines identified in Figs. 1 and 2 and the above artifacts from the experimental conditions, all lines in these patterns could be attributed to either the A2, B2 or $L2_1$ structures.

In Figs. 1(a) and 2(a), the Co_2FeSi and Co_2MnSi films with the same 55 nm thickness were grown on MgO (100) single crystal substrates. The Co_2MnSi (400) peak $(2\theta = 65.78^\circ)$ indicates the ordering of that material in the $L2_1$ structure. The weak Co_2MnSi (200) peak $(2\theta = 31.6^\circ)$ indicates the presence of Co-Fe antisite disorder [17]. Note, the Co_2MnSi (400) and Co_2FeSi (400) peaks are very strong in these spectra, while the Co_2FeSi and Co_2MnSi (200) reflections are weak, indicating these layers possess the $L2_1$ or B2 structure. As the annealing temperature increased, the intensities of the (400) and (200) peaks increased demonstrating a sequential improvement in the crystal order during annealing at high temperatures. The $L2_1$ and B2 structures of Co_2FeSi and Co_2MnSi should have coherent interfaces with the MgO (100) crystal which should enable coherent electron tunneling through the MgO and result in a giant TMR effect.

Figs. 1(b) and 2(b) show the XRD patterns of the 55 nm thick Co_2FeSi and Co_2MnSi films deposited on SiO_2 substrates for both the as-deposited and annealed samples. The clear (220) peak from the Co_2FeSi and Co_2MnSi films may suggest that an A2 structure was formed for both Heusler alloys films on annealing. In Fig. 2(b) Co_2MnSi (200) and (400) peaks are shown in the 400°C, 500°C and 600°C patterns which means that the B2 phase appears when the Co_2MnSi deposited on the Si\$SiO_2$substrate is annealed at elevated temperatures. But we do not find the presence of any B2 phase in the Co_2FeSi deposited on Si/SiO2 either in the as deposited condition or after any high temperature annealing. Also interesting from Fig. 2(b) is the fact that Co_2MnSi grows amorphous on Si/SiO_2 while

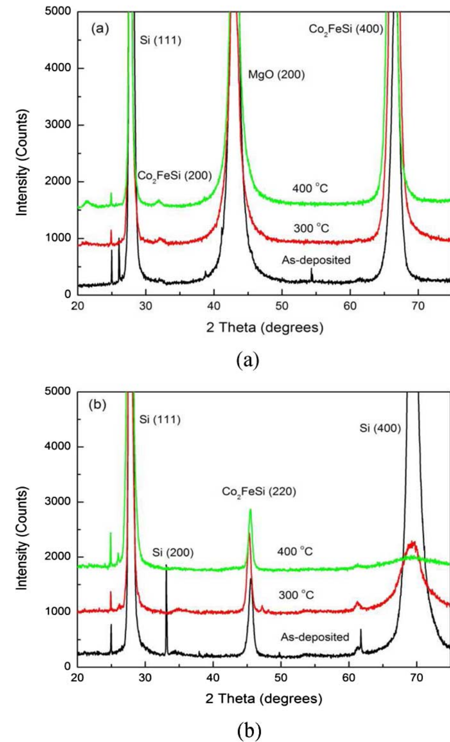

Fig. 1. (a) XRD patterns of 55 nm thick Co_2FeSi deposited on a MgO (100) substrate and heat treated at the indicated temperatures. (b) XRD patterns of 55 nm thick Co_2FeSi deposited on a Si/SiO_2 substrate and heat treated at the indicated temperatures.

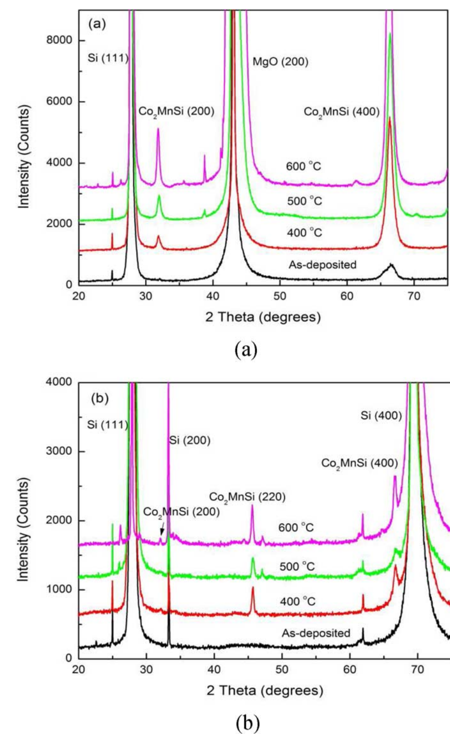

Fig. 2. (a) XRD patterns of 55 nm thick Co_2MnSi deposited on a MgO (100) substrate and heat treated at the indicated temperatures. (b) XRD patterns of 55 nm thick Co_2MnSi deposited on a Si\SiO_2 substrate and heat treated at the indicated temperatures.

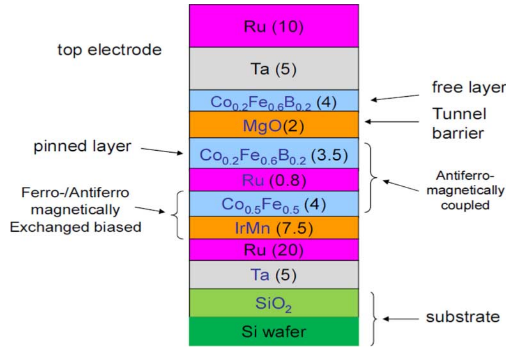

Fig. 3. Stack for the standard $MgO/Co_{20}Fe_{60}B_{20}$ MTJ.

isomorphous Co_2FeSi grows in the A2 crystalline structure on the Si/SiO_2 substrate.

The Co_2FeSi and Co_2MnSi cube edge is thought to grow at an angle of 45 degree with respect to an in-plane MgO (100) direction [8]. If this is the case, then there is only a 5% misfit between the MgO (100) lattice and that for either Co_2FeSi or Co_2MnSi. Consequently, epitaxial growth of Co_2FeSi or Co_2MnSi on MgO (100) would be expected and that is consistent with the strong texture observed for the Co_2FeSi and Co_2MnSi deposits shown in Fig. 1(a) and Fig. 2(a) respectively.

From the XRD spectra above we calculated the grain size of the Co_2FeSi or Co_2MnSi deposits on both the MgO (100) and Si/SiO_2 substrates after deposition and after annealing at the various temperatures. The as-deposited grain sizes for the Co_2FeSi on either substrate, and the Co_2MnSi deposited on the MgO (100) and Si/SiO_2 substrates were 15, 13, and 31 nm respectively. In all cases the grain size increased with annealing (increasing with the value of the annealing temperature) as expected. We do not have any information of the surface roughness of the layers other than to say it cannot be too large or the TMR values listed below would have been much smaller. The lattice constants for cubic Co_2FeSi and Co_2MnSi were determined to be 0.5653 nm and 0.5622 nm respectively. The cubic lattice constant of MgO (100) is 0.41985 nm.

Fig. 3 shows the typical stack structure of our MTJs with an MgO barrier and $Co_{20}Fe_{60}B_{20}$ ferromagnetic layers. In this structure, the 7.5 nm IrMn\4 nm CoFe\0.8 nm Ru\3.5 nm $Co_{20}Fe_{60}B_{20}$ portion of the stack acts as the reference layer. The free layer is the 4 nm $Co_{20}Fe_{60}B_{20}$. The 5 nm Ta\10 nm Ru acts as a capping layer.

The reasonably high measured TMR of the $Co_{20}Fe_{60}B_{20}$\MgO\$Co_{20}Fe_{60}B_{20}$ stack of 230% indicates the interfaces between $Co_{20}Fe_{60}B_{20}$\MgO\$Co_{20}Fe_{60}B_{20}$ are enabling a significant degree of coherent tunneling.

From Table I, the following observations can be made

1) if Co_2FeSi is deposited as the reference layer and the free layer is $Co_{20}Fe_{60}B_{20}$, the MTJ TMR is only 20%;
2) Iif 0.4 nm $Co_{20}Fe_{60}B_{20}$ is inserted between the Co_2FeSi and the MgO barrier (e.g., the Co_2FeSi\0.4 nm $Co_{20}Fe_{60}B_{20}$\MgO\$Co_{20}Fe_{60}B_{20}$ sample), the TMR ratio can be increased to 41%;
3) Iif 0.4 nm $Co_{20}Fe_{60}B_{20}$ is inserted between the MgO and the Co_2FeSi free layer (e.g., the $Co_{20}Fe_{60}B_{20}$\MgO\0.4 nm $Co_{20}Fe_{60}B_{20}$\Co_2FeSi sample) the TMR ratio is still just 41%.

TABLE I
THE TMR RATIO OF MTJS WITH Co_2FeSi AND Co_2MnSi DEPOSITED BELOW AND ABOVE THE MGO BARRIER LAYER

Stack structure on top of the 0.8 nm Ru of Figure 3	TMR %
$Co_{20}Fe_{60}B_{20}$(3.5 nm)\MgO\$Co_{20}Fe_{60}B_{20}$(4 nm)	230
$Co_{20}Fe_{60}B_{20}$(3.5 nm)\MgO\Co_2MnSi(4 nm)	29
Co_2FeSi(3.5 nm)\MgO\ $Co_{20}Fe_{60}B_{20}$(4 nm)	20
$CoFe_2Si$(3.5 nm)\ $Co_{20}Fe_{60}B_{20}$(0.4 nm)\MgO\ $Co_{20}Fe_{60}B_{20}$(4 nm)	41
$Co_{20}Fe_{60}B_{20}$(3.5 nm)\MgO\ $Co_{20}Fe_{60}B_{20}$(0.4 nm)\Co_2FeSi(4 nm)	41
$Co_{20}Fe_{60}B_{20}$(3.5 nm)\MgO\ $Co_{20}Fe_{60}B_{20}$(0.8 nm)\Co_2FeSi(4 nm)	116
$Co_{20}Fe_{60}B_{20}$(3.5 nm)\MgO\Co_2FeSi(4 nm)	150
$Co_{20}Fe_{60}B_{20}$(3.5 nm)\MgO\$CoFe_2Si$(4 nm)	94

From these three observations, one can conclude Co_2FeSi cannot form the $L2_1$ or the B2 structure on either Ru or $Co_{20}Fe_{60}B_{20}$. This is concluded from the low TMR values of the above configurations since only $L2_1$ or B2 structures have interfaces with the MgO (100) that enable good coherent tunneling and high TMR values.

Three further observations can be made from Table I as follows:

1) Increasing the thickness of the $Co_{20}Fe_{60}B_{20}$ to 0.8 nm (e.g., the $Co_{20}Fe_{60}B_{20}$MgO\0.8 nm\Co_2FeSi sample), results in an increase in the TMR ratio to 116%. In this case the $Co_{20}Fe_{60}B_{20}$ may be forming a continuous layer. There is good tunneling through the $MgO/Co_{20}Fe_{60}B_{20}$ interface, and the Co_2FeSi just contributes additional magnetization.
2) If the Co_2FeSi is deposited directly on top of the MgO barrier layer and acts as the free layer (e.g., the 3.5 nm $Co_{20}Fe_{60}B_{20}$\MgO\4 nm Co_2FeS sample), the TMR ratio can be as high as 150%. This result is close to the TMR ratio of that using $Co_{20}Fe_{60}B_{20}$ as the free layer, implying the Co_2FeSi can grow on top of the MgO (100) barrier layer [18] in the $L2_1$ structure.
3) When the 4 nm thick Co_2MnSi layer is deposited on the top of the MgO(100) barrier as the free layer, the TMR ratio is 29%. It is much lower than the TMR ratio of Co_2FeSi as free layer. Due to the similarity in the growth of Co_2FeSi and Co_2MnSi, it is quite likely that even in this latter case the crystal structure of the Co_2MnSi is B2. The reason for the low TMR ratio may come from the interdiffusion of Mn into the MgO layer [19].

IV. CONCLUSION

In conclusion, we found that Co_2FeSi and Co_2MnSi form in either the $L2_1$ or B2 structures when grown on the top of an MgO (100) barrier layer. Otherwise Co_2FeSi and Co_2MnSi will grow with the A2 structure. The $L2_1$ or B2 structures of the Heusler alloy film will enable coherent electron tunneling across the interface with the MgO barrier and result in a high TMR value. When Co_2FeSi is adjacent to a Ru or $Co_{20}Fe_{60}B_{20}$ layer, it will form in an A2 structure and the TMR will be lower. Low TMR values found in a $Co_{20}Fe_{60}B_{20}$ (3.5 nm)\MgO\Co_2MnSi(4 nm) sample may be due to Mn diffusion into the MgO.

ACKNOWLEDGMENT

The authors would like to thank Dr. A. Davydov, Dr. S. Y. Zheng, Dr. I. Levin, and Mrs. M. Williams at NIST for helpful discussions on the analysis of our X-ray diffraction data.

REFERENCES

[1] R. A. de Groot, F. M. Mueller, P. G. van Engen, and K. H. J. Buschow, “New class of materials: Half-metallic ferromagnets,” *Phys. Rev. Lett.*, vol. 50, pp. 2024–2027, 1983.

[2] S. Ishida, S. Fujii, S. Kashiwagi, and S. Asano, “Search for half-metallic compounds in Co2MnZ (Z = IIIb, IVb, Vb element),” *J. Phys. Soc. Japan*, vol. 64, pp. 2152–2157, 1995.

[3] I. Galanakis, P. H. Dederichs, and N. Papanikolaou, “Slater-Pauling behavior and origin of the half-metallicity of the full-Heusler alloys,” *Phys. Rev. B*, vol. 66, p. 174429, 2002.

[4] S. Yuasa, T. Nagahama, A. Fukushima, Y. Suzuki, and K. Ando, “Giant room-temperature magnetoresistance in single-crystal Fe/MgO/Fe magnetic tunnel junctions,” *Nature Mater.*, vol. 3, pp. 868–871, 2004.

[5] S. Yuasa, A. Fukushima, H. Kubota, Y. Suzuki, and K. Ando, “Giant tunneling magnetoresistance up to 410% at room temperature in fully epitaxial Co/MgO/Co magnetic tunnel junctions with bcc Co(001) electrodes,” *Appl. Phys. Lett.*, vol. 89, p. 042505, 2006.

[6] S. S. Parkin, C. Kaiser, A. Panchula, P. M. Rice, B. Hughes, M. Samant, and S. H. Yang, “Giant tunnelling magnetoresistance at room temperature with MgO (100) tunnel barriers,” *Nature Mater.*, vol. 3, pp. 862–867, 2004.

[7] D. Djayaprawira, K. Tsunekawa, M. Nagai, H. Maehara, S. Yamagata, N. Watanabe, S. Yuasa, Y. Suzuki, and K. Ando, “230% room-temperature magnetoresistance in CoFeB/MgO/CoFeB magnetic tunnel junctions,” *Appl. Phys. Lett.*, vol. 86, p. 092502, 2005.

[8] S. Trudel, O. Gaier, J. Hamrle, and B. Hillebrands, “Magnetic anisotropy, exchange and damping in cobalt-based full Heusler compounds: An experimental review,” *J. Phys. D: Appl. Phys.*, vol. 43, p. 19300, 2010.

[9] T. Grad, S. S. Parkin, and C. Felser, “Heusler compounds—A material class with exceptional properties,” *IEEE Trans. Magn.*, vol. 47, no. 2, p. 367, Feb. 2011.

[10] S. Tsunegi, Y. Sakuraba, M. Oogane, K. Takanashi, and Y. Ando, “Large tunnel magnetoresistance in magnetic tunnel junctions using a Co_2MnSi Heusler alloy electrode and a MgO barrier,” *Appl. Phys. Lett.*, vol. 93, p. 112506, 2008.

[11] E. Ozawa, S. Tsunegi, M. Oogane, H. Naganuma, and Y. Ando, “The effect of inserting thin Co_2MnAl layer into the Co_2MnSi/MgO interface on tunnel magnetoresistance effect,” *J. Phys.*, vol. 266, p. 012104, 2011, confer series.

[12] W. Wang, E. Liu, M. Kodzuka, H. Sukegawa, M. Wojcik, E. Jedryka, G. H. Wu, K. Inomata, S. Mitani, and K. Hono, “Coherent tunneling and giant tunneling magnetoresistance in Co_2FeAlÕMgOÕCoFe magnetic tunneling junctions,” *Phys. Rev. B*, vol. 81, p. 140402, 2010.

[13] N. Tezuka, N. Ikeda, F. Mitsuhashi, and S. Sugimoto, “Improved tunnel magnetoresistance of magnetic tunnel junctions with Heusler $Co_2FeAl_{0.5}Si_{0.5}$ electrodes fabricated by molecular beam epitaxy,” *Appl. Phys. Lett.*, vol. 94, p. 162504, 2009.

[14] Z. Wen, H. Sukegawa, S. Mitani, and K. Inomata, “Tunnel magnetoresistance in textured Co_2FeAl/MgO/CoFe magnetic tunnel junctions on a Si/SiO_2 amorphous substrate,” *Appl. Phys. Lett.*, vol. 98, p. 192505, 2011.

[15] T. Ishikawa, S. Hakamata, K. Matsuda, T. Uemura, and M. Yamamoto, “Fabrication of fully epitaxial Co_2MnSi/MgO/Co_2MnSi magnetic tunnel junctions,” *J. Appl. Phys.*, vol. 103, p. 07A919, 2008.

[16] The manufacturer names are used here to more properly describe the experimental conditions, and in no way does it constitute an endorsement by the authors or the National Institute of Standards and Technology.

[17] Anupam, P. C. Joshi, P. K. Rout, Z. Hossain, and R. C. Budhani, “Charge transport and magnetic ordering in laser ablated Co_2FeSi thin films epitaxially grown on (100) $SrTiO_3$,” *J. Phys. D: Appl. Phys.*, vol. 43, p. 255002, 2010.

[18] K. Tsunekawa, D. D. Djayaprawira, M. Nagai, H. Maehara, S. Yamagata, N. Watanabe, S. Yuasa, Y. Suzuki, and K. Ando, “Giant tunneling magnetoresistance effect in low-resistance CoFeB/MgO(001)/CoFeB magnetic tunnel junctions for read-head applications,” *Appl. Phys. Lett.*, vol. 87, p. 072503, 2005.

[19] J. Hayakawa, S. Ikeda, Y. M. Lee, F. Matsukura, and H. Ohno, “Effect of high annealing temperature on giant tunnel magnetoresistance ratio of CoFeB/MgO/CoFeB magnetic tunnel junctions,” *Appl. Phys. Lett.*, vol. 89, p. 232510, 2006.